Energy 276 (2023) 127551

Contents lists available at ScienceDirect

Energy

journal homepage: www.elsevier.com/locate/energy

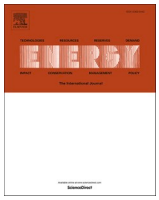

Assessment of the interchangeability of coal-biomass syngas with natural gas for atmospheric burners and high-pressure combustion applications

Daniel A. Quintero-Coronel [a,b], Adalberto Salazar [c], Oscar R. Pupo-Roncallo [d], Antonio Bula [d], Lesme Corredor [d], German Amador [c], Arturo Gonzalez-Quiroga [d,*]

[a] Department of Mechanical Engineering, Universidad del Norte, Barranquilla, 080001, Colombia
[b] GITYD Research Unit, Department of Mechanical Engineering, Universidad Francisco de Paula Santander, Ocaña, Colombia
[c] Grupo de Investigación de Motores y Combustibles Alternativos, Departamento de Ingeniería Mecánica, Universidad Técnica Federico Santa María, Avenida España 1680, Valparaíso, Chile
[d] UREMA Research Unit, Department of Mechanical Engineering, Universidad del Norte, Barranquilla, 080001, Colombia

ARTICLE INFO

Handling Editor: Krzysztof (K.J.) Ptasinski

Keywords:
Gas industry
Gas quality
Combustion performance
Flame stability
Methane number
Wobbe index

ABSTRACT

Syngas from biomass-coal co-gasification represents a viable energy vector to incorporate alternative energy sources into electricity production and industrial heating. Although the low energy content of syngas hinders its use, syngas-natural gas blends could overcome this challenge. This study assesses syngas-natural gas interchangeability in atmospheric burners via the combustion potential and the corrected Wobbe index according to Delbourg's approach. Likewise, this research evaluates methane number as an interchangeability indicator for high-pressure combustion. The syngas originated from a Top-Lit UpDraft gasifier, using coal-biomass blends of 0–100, 25–75, and 45–55 wt %, with air as the gasifying agent. The syngas featured a Lower Heating Value ranging from 3.0 to 3.8 MJ Nm-3. Results based on Delbourg's approach indicated that syngas-natural gas blends of up to 15 vol % syngas could operate in atmospheric natural gas burners without modifications. Furthermore, the methane number for syngas-natural gas blends of 15 vol % syngas was 5.8% higher than that of natural gas. The results show slight variations in flue gas composition, adiabatic flame temperature, and laminar flame velocity between natural gas and syngas-natural gas blends. The study showcases the potential of using syngas-natural gas blends in thermal applications and identifies key areas for further research.

1. Introduction

Globally, the combustion of natural gas (NG) generates a vast amount of thermal energy, which is utilized in industrial processes such as ceramic, cement, paper, and electricity production [1–4]. Partially replacing NG with syngas from the gasification of carbon-based feedstock, including biomass, is a plausible alternative [5]. This study evaluates the partial substitution of NG with syngas obtained from the co-gasification of coal and biomass in a Top-Lit Updraft (TLUD) gasifier. An interchangeability analysis based on Delbourg's approach was conducted to determine the maximum share of syngas that could be used in existing atmospheric burners [6]. We also estimated flue gas composition, adiabatic flame temperature (T_{adb}), and laminar flame velocity (S_L). Finally, the study was extended to high-pressure combustion applications through the determination of the methane number (*MN*), to evaluate the autoignition propensity of syngas-NG blends.

The co-gasification of biomass and coal produces syngas while taking advantage of the high reactivity of biomass and the high energy content and availability of coal. Syngas mainly contains CO, H_2, CH_4, and CO_2, but also includes N_2 when air is used as the gasification agent. Fixed and fluidized bed gasifiers are used to co-gasify coal and biomass [7]. This study uses a TLUD fixed bed gasifier, an inverted or reversed downdraft [8,9]. The Low Heating Value (*LHV*) of syngas from TLUD gasifiers operating with air could range from 3.7 to 5.6 MJ Nm^{-3}, similar to the *LHV* of syngas from downdraft and updraft fixed bed gasifiers [10,11]. However, compared with natural gas, the syngas from the TLUD gasifier has a relatively low energy content, making it unsuitable for direct use in large thermal applications for direct heating or electricity generation. Replacing NG with low-*LHV* syngas is, therefore, challenging. However, co-firing NG and syngas without modifying the combustor is a promising option [12]. Thus, it is crucial to determine the share of syngas that can be co-fired with NG while avoiding or minimizing modifications to industrial processes that primarily use natural gas as a fuel.

* Corresponding author.
E-mail address: arturoq@uninorte.edu.co (A. Gonzalez-Quiroga).

https://doi.org/10.1016/j.energy.2023.127551
Received 2 November 2022; Received in revised form 14 April 2023; Accepted 16 April 2023
Available online 20 April 2023

Nomenclature

a	Correction coefficient for individual hydrocarbons
a_s	Semi-range (or half-width) between the upper and lower limits
AGA	American Gas Association
C	Mass percentage of atomic carbon in the feed, wt %
CCE	Carbon conversion efficiency
CFD	Computational Fluid Dynamic
C_{pot}	Combustion potential
dafb	Dry-ash-free basis
db	Dry basis
d_r	Relative density
FC	Fixed carbon, wt %
GT	Gas turbine
HVBC	High-volatile bituminous coal
HHV_F	Higher heating value of feedstock, kJ kg^{-1}
HHV_g	Higher heating value of gas, MJ Nm^{-3}
ICE	Internal combustion engine
IW	Wobbe index, MJ Nm^{-3}
IW_c	Corrected Wobbe index, MJ Nm^{-3}
K_1	Corrected factor 1
K_2	Corrected factor 2
LHV_g	Lower Heating Value of gas, MJ Nm^{-3}
MN	Methane number
n	The number of measurements in the experimental set
NG	Natural Gas
PKS	Palm Kernel Shell
S	Standard deviation
S_L	Laminar flame velocity, m s^{-1}
T	Temperature, K
T_{adb}	Adiabatic flame temperature, K
TLUD	Top-lit updraft
U	Gas factor 1
u_A	Estimated uncertainty type A
u_A	Estimated uncertainty type B
u_f	Ignition front propagation velocity, mm s^{-1}
v	Gas factor 2
v_s	Superficial air velocity, cm s^{-1}
VM	Volatile matter, wt %
β	Regression coefficient
y_i	Molar fraction of compound i
Φ	Equivalence ratio

There are graphical and analytical methods to evaluate the interchangeability of gaseous fuels [6]. Some authors have used these methods; for example, Honus et al. [13] used analytical multi-index interchangeability methods to show that fuel gases from polyvinyl chloride pyrolysis at 973 K are suitable for NG burners, reaching Wobbe indexes (IW) between 50 and 54 MJ Nm^{-3}. The multi-index interchangeability methods represent indexes developed by various organizations to evaluate gas interchangeability at different conditions, including the Knoy index, Dutton factors, AGA indexes, and Weaver indexes. The AGA indexes evaluate the degree of fuel substitution by considering phenomena such as lifting, flashback, and yellow-tip flames of the original gas and its substitute [14]. The Weaver indexes include variables to evaluate changes in primary aeration, flashback flame, heat rate generation, lifting flame, yellow tip formation, and incomplete combustion [6,14–16].

In this study, we employ Delbourg's graphical approach to assess the interchangeability of NG in atmospheric burners. This method utilizes two variables, the corrected Wobbe index (IW_c) and the combustion potential (C_{pot}). The corrected Wobbe index is obtained by multiplying IW by two correction factors defined in Ref. [6], while the combustion potential relates to the fuel's combustion velocity and stability (flame lifting and flame flashback) [13]. Delbourg's approach only evaluates the interchangeability of gases in atmospheric burners, which typically operate at gauge pressures in the range of 0.5–3 kPa and are commonly used in domestic and small-scale industrial processes [17]. To complement the results obtained through Delbourg's approach, we also estimated the flue gas composition, T_{adb}, and S_L at different equivalence ratios.

Accurate estimation of S_L is essential for integrating low calorific gaseous fuels into combustion processes as their chemical composition differs from that of natural gas. S_L provides information on flame stability and propagation in a combustion device, indicating turbulent flames [18]. It is also used in gas engine design, turbulent premixed flames modeling, and chemical reaction mechanisms validation [19]. Some studies have evaluated the behavior of the S_L of gaseous fuels under different conditions. Richter et al. [20] measured S_L values of different CH_4–H_2–N_2 and H_2–N_2 blends using the cone angle method with air as the oxidizer. Their results reveal a notable increase in S_L as the H_2 content increased. Papafilippou et al. [21] found *via* simulation that syngas combustion reduced the swirl intensity of a TECFLAM burner designed for NG. Vieira et al. [22] reported S_L values of 0.23–0.33 m s^{-1} for a syngas with a chemical composition (vol %) of 20% CO, 16% H_2, and 1.8% CH_4; the remainder being CO_2 and N_2. Munajat et al. [19] observed that S_L is affected by adding H_2O and C_2H_6 to the simulated syngas (CO, H_2, CH_4, CO_2, and N_2), highlighting the need for further investigation into the impact of tar on S_L.

Calculating MN, in addition to S_L, is necessary to determine the interchangeability conditions of gaseous fuels in high-pressure combustion devices such as gas turbines and reciprocating engines. Thus, we evaluated MN of syngas, NG, and its blends as an interchangeability indicator for high-pressure combustion applications.

The methane number is a key parameter in determining the knock resistance of fuel gases in internal combustion engines [23], which can prevent structural damage [24]. Malenshek et al. [25] experimentally determined methane numbers for simulated fuel gases. Their study showed that syngas from coal, with an average chemical composition (vol %) of 16.3% N_2, 1% CO_2, 24.8% H_2, and 58% CO, here named coal gas 1, and coal gas 2 with 7% CH_4, 6% CO_2, 44% H_2, and 43% CO, feature MNs of 30 and 23.9, respectively; while syngas from wood gasification, with 10% CH_4, 3% N_2, 23% CO_2, 40% H_2, and 24% CO, here named wood gas 1, and wood gas 2 with 1% CH_4, 35% N_2, 15% CO_2, 31% H_2, and 15% CO, presented methane numbers of 61.5 and 70.2, each. Wise et al. [26] observed that MN increased as the H_2 and CO contents were higher. The authors observed that producer gases with a shorter flame initiation period tend to knock faster, indicating that S_L correlates with MN and early flame development. Some studies report that most engines present the best fuel efficiency for MNs higher than 80. Nevertheless, these engines also can work at lower MNs values, but at reduced efficiency [27]. In addition, internal combustion engines require modifications in the compression ratio and ignition timings for MN between 35 and 60 to operate without knocking [28].

The interchangeability of syngas-NG blends using Delbourg's approach remains understudied. Studies have explored the substitution of NG with other gaseous fuels in various industrial processes, including burners in industrial furnaces, household applications, and high-pressure combustion devices (mainly internal combustion engines). For instance, Kiedrzyńska et al. [12] found that a 10% share of syngas with an energy content of 4.1–4.8 MJ m^{-3} (21% CO, 14% H_2, 12% CO_2, 3% CH_4, 1% O_2, and 49% N_2, vol %) could operate in a burner without modifications. However, higher shares of syngas resulted in failed

combustion. Similarly, Gómez et al. [1] performed CFD simulations comparing the co-firing of NG and syngas from three biomasses and three off-process gases in a burner used in the ceramic industry. They found that changes to the burner geometry may be necessary, which poses an additional obstacle to implementing syngas-NG co-firing [1, 12].

On the other hand, Caligiuri et al. [29] experimentally evaluated the addition of syngas at different percentages in an NG internal combustion engine by considering four spark ignition timings (10°, 25°, 35° and 45° before the top dead center). The results showed that this mixture reduced power output by about 6% and the amount of NO_x produced in the combustion process. As reported in other studies, the NO_x reduction was linked to the presence of CO_2 and N_2 in the syngas [30]. Kohn et al. [31] noted that adding 5% of syngas (H_2/CO) to a simulated landfill gas (50% CH_4, 50% CO_2, vol%) reduced the CO emission in a four-stroke Honda GC160E, which was associated with the enhancement of reactive in the mixture due to H_2 content in the syngas. Changwei et al. [32] indicated that the syngas addition enhanced the gasoline burn, which was associated with high S_L values and wide flammability ranges of syngas because of H_2 and CO contents.

Zarenezhad [33] conducted CFD simulations to study the impact of changing the compression ratio (10.50, 11.05, 11.80) on gasoline and NG enriched with 10% H_2 as fuels in an engine. The results showed that output power increased when the compression ratio was 11.80, without significant changes in NO_x emissions for NG enriched with H_2 as fuel compared with gasoline. Nadaleti et al. [34] observed reductions in NO_x emissions in a spark ignition engine fueled with syngas, compared to natural gas and biogas (65 vol % CH_4) operation at lean combustion conditions, a trend also observed by Changwei et al. [32] in a hybrid syngas-gasoline engine. In addition, the study [34] showed an increase in the heat release rate in the engine because of the high S_L associated with the H_2 content of syngas.

The addition of syngas in compression ignition engines has been studied through diverse strategies. Olanrewaju et al. [35] used a Heat Release Rate model to study the substitution of diesel with syngas in a dual-fuel engine. They found that as the share of syngas increased, ignition delay increased, delaying the start of combustion and decreasing peak pressure and peak heat release rate compared to pure diesel operation. Krishnamoorthi et al. [36] examined the combination of syngas and biodiesel in a conventional single-cylinder direct-injection diesel engine using experiments and CFD simulations. A 25% energy share of syngas resulted in lower emissions than diesel operation, reducing hydrocarbon, particle matter, and NO_x emissions by 29%, 77%, and 22%, respectively. The study concluded that syngas is a promising fuel for use in stationary compression ignition engines.

As aforementioned, diverse studies have explored the syngas use along with other fuels, such as NG, gasoline, and diesel, following different strategies to integrate the syngas for various purposes, boarding combustion devices working at diverse operating conditions. However, to the best of the authors' knowledge, the interchangeability of natural gas with syngas derived from the co-gasification of coal and biomass has been under-explored. In addition, the purpose of using *MN*, C_{pot}, and the IW_c on the Delbourg diagram to evaluate the interchangeability of syngas-natural gas mixtures in high-pressure combustion applications remains unexplored. Hence, the results of this study could provide insights into the potential of syngas-natural blends to operate in atmospheric natural gas burners and high-pressure combustion devices.

2. Materials and methods

This section describes the TLUD setup and the coal and biomass used for co-gasification experiments. Then, we present Delbourg's approach for evaluating syngas-natural gas interchangeability in atmospheric burners. The section also describes *MN* calculations and the correlation model for estimating the syngas methane number. The section finalizes with a description of the uncertainty analysis.

2.1. Syngas from coal-biomass Co-gasification process

Fig. 1 shows a schematic representation of the TLUD gasifier, which is comprised of a cylinder with an inner diameter of 152.4 mm and a height of 900 mm. The gasifier has a 25 mm thick insulation layer with a thermal conductivity of $0.044 Wm^{-1}K^{-1}$. Air enters from the bottom of the gasifier through a 63.5 mm line connected to a 600 W blower (model STPT600-B3, Stanley) that regulates the air mass flow rate. A flow sensor model 8455-TSI measures air velocity. At the same time, six K-type thermocouples, with a sensitivity of 41 μV/°C spaced every 100 mm on the axial axis of the gasifier, provide the temperature profile, which enables the estimation of the ignition front propagation velocity (u_f). Air velocity and temperature are recorded and displayed using a customized LabView interface. Figure S2.1 in the supplementary material shows a picture of the gasification setup.

The feedstock consists of Palm Kernel Shell (PKS), a byproduct of the palm oil process, and High Volatile Bituminous Coal (HVBC). The experimental stage involved a 3^2-factorial design, evaluating the influence of air-superficial velocity (v_s), with values of 6.90 (±0.22), 8.20 (±0.26), and 9.60 (±0.25) cm s^{-1}, with the parenthesis terms representing the estimated uncertainty (section 2.4), and coal mass percentage (MP_c), with shares of 0%, 25%, and 45% on the ignition front propagation velocity estimated from Equation (1). The 3^2-factorial design results in nine runs. Adding one replicate gives a total of 18 runs for evaluating variables.

The ignition front propagation velocity measures the stability and uniformity of the TLUD operation. This parameter represents the velocity at which drying, pyrolysis, oxidation, and reduction fronts occur [37]. In Equation (1), u_f is a function of the ΔX, which represents the distance between two thermocouples, and the time interval $(t_{j+1} - t_j)$ corresponding to temperatures T_j and T_{j+1} when thermocouples reach 723 K. On the other hand, in the experiments, the particle size of PKS had a mean value of 4.9 mm, with a standard deviation of ±2.3 mm, while HVBC had a sieve fraction between 4.7 and 9.5 mm. Likewise, the moisture fraction for these feedstocks was 6.0 and 2.0 % wt for PKS and HVBC, respectively.

$$u_f = \frac{\Delta X}{t_{j+1} - t_j} \tag{1}$$

A typical experiment in the TLUD gasifier initiates with introducing the PKS, HVBC, or their blends at defined experimental conditions in the gasifier chamber until reaching about 700 mm of height. For blends of PKS and HVBC, graduated cylindrical tubes enable measuring the amount required to later pass to a container, mixed by 2 min, and then transferred manually to the reactor. As the feedstock enters the gasifier, the corresponding thermocouple is introduced, which avoids the formation of empty pockets or channeling into the reactor. Then, the v_s is adjusted, reaching the set point, and a part of the feedstock in the upper part of the gasifier is soaked with mineral diesel and ignited with a torch. Thus, the gasifier works in batch mode until it consumes all feedstock.

In the experiment, when the first thermocouple reaches the peak temperature, the gas measurement begins using the micro-GC (Model 490, Agilent Technologies, Inc), equipped with three channels that incorporate thermal conductive detectors, measuring CH_4, C_2H_6, C_3H_8, N_2, CO, CO_2, and H_2. Figure S2.2 in the supplementary material shows a typical temperature profile obtained in the TLUD gasifier. The chromatograph registers measurements every 3 min. The sampling gas passes by a bubbling bottle, a cotton filter, and a vacuum pump, which releases the gas sample in a second bubbling bottle connected to the chromatograph. Experiments do not include tar measurements, representing a future research topic in the TLUD gasifier. The syngas obtained in TLUD gasifiers passes through a bed of char and ashes at high temperatures, which could help to reduce the tar content. This reduction

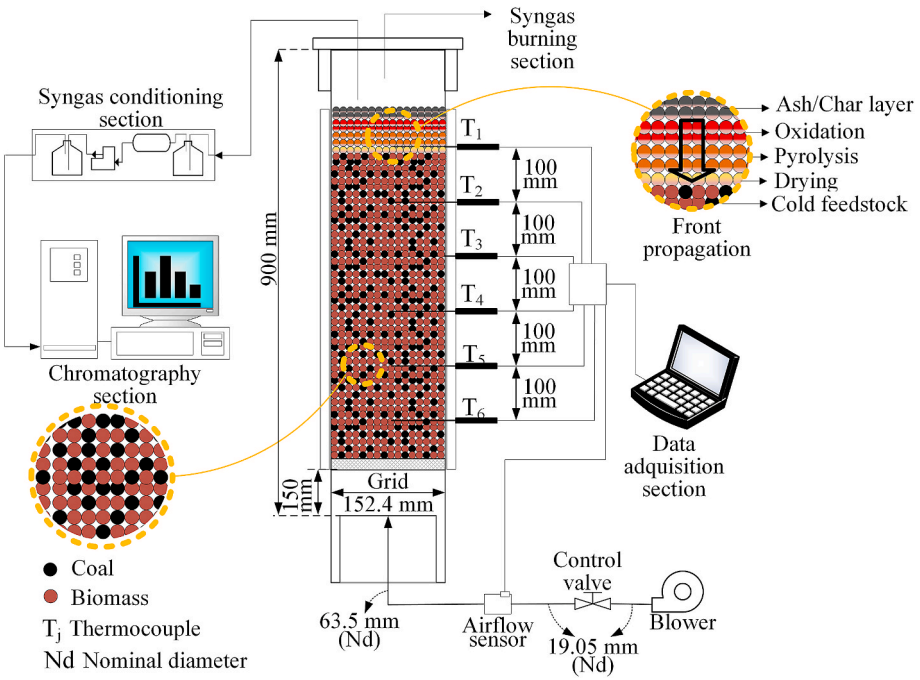

Fig. 1. Schematics of the TLUD fixed bed gasifier for the co-gasification of coal and biomass. Modified from Ref. [38].

only is possible as the char and ash are formed in the gasification process.

The co-gasification of coal and biomass using air yields significant concentrations of H_2, CO, CO_2, H_2O, and N_2, the latter with values higher than 50 vol %, because of the high N_2 content in the air. Equations (2) and (3) determine the Lower Heating Value (LHV_g) and the Higher Heating Value (HHV_g) of the syngas.

$$LHV_g = \left(12.63y_{CO} + 10.78y_{H_2} + 35.88y_{CH_4}\right)\ \left(\text{MJ Nm}^{-3}\right) \tag{2}$$

$$HHV_g = \left(12.63y_{CO} + 12.74y_{H_2} + 39.81y_{CH_4}\right)\ \left(\text{MJ Nm}^{-3}\right) \tag{3}$$

where y_{CO}, y_{CH_4}, y_{H_2} are the molar fractions of the syngas. The constant values represent the *LHV* and the *HHV* at standard conditions (273.15 K and 101.325 kPa) for CO, CH_4, and H_2, respectively [39].

2.2. Gas interchangeability for atmospheric burners

ISO standard 13,686 [6] describes different methods to evaluate gas interchangeability. This study uses Delbourg's approach [6], a graphics-based technique, to measure the degree of fuel gas substitution in industrial or household burners, estimating the maximum share of substitute gas that does not affect the operating conditions of the burner.

The Wobbe index, the ratio between the *HHV* of the fuel and the square root of its relative density (d_r) regarding air at the same reference conditions, measures the heat input of a burner. Hence, two fuel gases with the same Wobbe index value provide the same thermal energy input [6]. Delbourg's approach uses IW_c, consisting of *IW*, multiplied by two correction factors, K_1 and K_2. The factor K_1 is a function of the sum of the heating value of hydrocarbons presents at concentrations higher than CH_4 [13], while K_2 considers the *HHV* of the substitute gas and the concentrations of CO, CO_2, and O_2. Delbourg's approach uses C_{pot}, related to the burning rate and combustion stability of the substitute gas. Equations (4)–(6) define *IW*, IW_c, and C_{pot}, respectively [6].

$$IW = \frac{HHV_g}{\sqrt{d_r}} \tag{4}$$

$$IW_c = K_1 K_2 IW \tag{5}$$

$$C_{pot} = U\left(\frac{y_{H_2} + 0.7y_{CO} + 0.3y_{CH_4} + v\sum a y_{C_nH_m}}{\sqrt{dr}}\right) \tag{6}$$

where y_{CO_2} and $y_{C_nH_m}$ are the molar fractions of CO_2 and hydrocarbons different from CH_4, respectively. The *U* and *v* parameters are correction factors that depend on the gas type [6,13]. In Equation (6), y_{CO_2}, $y_{C_nH_m}$, y_{H_2}, and y_{CO} should be multiplied by 100, or expressed in % vol.

2.3. Interchangeability for high-pressure combustion applications

In addition to ensuring the interchangeability of gaseous fuels, it is essential to guarantee that the substitute fuel will not auto-ignite in devices such as gas turbines (GTs) and internal combustion engines (ICEs). In particular, the stringent and varied operating conditions in ICEs require complementary analyses to evaluate fuel substitution in these devices because any change in fuel composition alters engine performance [40]. This work used *MN* as a complementary metric to IW_c and C_{pot}. This metric is analogous to the octane number widely used to characterize the knock propensity of liquid fuels. The methodology estimates the knock resistance of a test fuel by comparing it with the knock resistance of a mixture of H_2 and CH_4, which work as reference fuels [41]. Even though the estimation of methane number for natural gas can use *MN* calculators [42], estimating this metric for other gases is not straightforward. A common approach consists of experiments and empirical correlations. This paper computed *MN* for NG and Syngas-NG blends, using the online calculator developed by Cummins [42], and the *MN* of syngas, using Equation (7). This equation was derived using experimental data reported in the literature with gas compositions similar to those employed in this work [25,26,43]

$$\begin{aligned} MN = {} & \beta_1 y_{N_2} + \beta_2 y_{CO_2} + \beta_3 y_{N_2} y_{CO_2} \\ & + \beta_4 y_{N_2} y_{CO} + \beta_5 y_{N_2} y_{H_2} + \beta_6 y_{N_2} y_{CH_4} + \beta_7 y_{CO} y_{CH_4} + \beta_8 y_{H_2} y_{CH_4} + \beta_9 y_{CO} y_{H_2} + \beta_{10} y_{N_2}^2 \end{aligned} \tag{7}$$

The regression coefficients β in Equation (7) are $\beta_1 = -21214$, $\beta_2 = 349$, $\beta_3 = 21560$, $\beta_4 = 21410$, $\beta_5 = 21070$, $\beta_6 = 21668$, $\beta_7 = 264$, $\beta_8 = 252$, $\beta_9 = -454$, and $\beta_{10} = 21377$.

2.4. Uncertainty analysis

In this study, we report on measured and calculated variables that are subject to various sources of uncertainty. We employed both Type A and Type B evaluations to estimate the uncertainty for the principal variables associated with the experimental setup. Type A evaluation calculates uncertainties for experimental values measurements of a required variable, while Type B evaluation considers all other forms of uncertainty. For Type B evaluation, we assessed uncertainty from the air velocity sensor, thermocouples, and the chromatograph device. Table S3.1 summarizes the technical specifications for these devices.

Equation (8) outlines the variables required for Type A uncertainty evaluation. In this equation, S is the standard deviation, n represents the number of measurements for a defined condition, and u_A is the estimated standard uncertainty of the mean value. Equation (9) details the variables used to calculate the uncertainty associated with Type B uncertainty evaluation (u_B). In this study, we assumed that values follow a rectangular distribution. Hence, a_s is the semi-range (or half-width) between the upper and lower limits [44]. Section S3 of the supplementary material provides two additional equations for estimating the combined uncertainty for measured or calculated terms with multiple uncertainty sources. The reported uncertainty reflects a confidence level of 95% with a coverage factor of 1.96.

$$u_A = \frac{S}{\sqrt{n}} \tag{8}$$

$$u_B = \frac{a_s}{\sqrt{3}} \tag{9}$$

3. Results and discussion

This section starts with a description of the properties of the feedstock, followed by syngas compositions. Next, we describe the gas interchangeability results and relevant parameters for syngas and NG combustion in atmospheric burners. Then, the outcomes associated with the *MN* estimation for syngas and NG, and their behavior regarding IW_c and C_{pot} are discussed.

3.1. Feedstock composition

Table 1 shows the proximate and ultimate analyses of PKS and HVBC, the feedstock used in the co-gasification process. The elemental composition is on a dry-ash-free basis (dafb), while the proximate analysis is on a dry basis (db). The coal used has higher carbon (C) content on a daf basis than PKS, while the opposite is true for the hydrogen (H) content. Similarly, PKS has 55% more oxygen (O) than HVBC. In addition, nitrogen (N) and sulfur (S), together, represent about two percent on a daf basis for both feedstocks. Proximate analysis indicates that HVBC has more Fixed Carbon (FC) and ash content than PKS, but lower Volatile Matter (VM). The volatile matter content in PKS exhibits a relatively high reactivity. Thus, biomass could enhance coal devolatilization in the co-gasification process while producing syngas with combined energy properties.

Table 1
Elemental composition on a dry-ash-free basis (dafb), proximate analysis on a dry basis (db), and higher heating value (*HHV*) of palm kernel shell (PKS) and high-volatile bituminous coal (HVBC).

Analysis/ parameter	Palm kernel shell, PKS [45]	High volatile bituminous coal, HVBC [46]
C, % wt dafb	53.8	74.6
H, % wt dafb	6.13	6.07
N, % wt dafb	0.88	0.05
S, % wt dafb	0.11	1.91
O, % wt dafb	39.0	17.4
Molar H/C ratio	1.36	0.97
Molar O/C ratio	0.54	0.18
VM, % wt db	81.6	33.7
FC, % wt db	14.6	45.4
Ash, % wt db	3.78	20.9
HHV_F, kJ/kg db	21,073[a]	25,781[b]

[a] Gaur and Reed correlation [47].
[b] Mason and Ghandi correlation [48].

3.2. Syngas composition

Table 2 shows the syngas composition derived from experimental tests in the TLUD gasifier [38]. The results indicate that 100% PKS yields syngas of higher LHV compared with tests using 25 and 45 wt % HVBC. Thiagarajan et al. [49] also observed similar trends in the co-gasification of PKS and bituminous coal in a downdraft gasifier with air as a gasification agent. Their results indicated that the energy content of the syngas varied between 1.5 and 2.3 MJ Nm^{-3}, with pure PKS gasification showing the best energy content, followed by tests with 50 wt % coal and 50 wt% PKS that reached an energy content of 2.2 MJ Nm^{-3}. Similarly, Thengane et al. [50] observed that co-gasification of high ash biomass and high ash coal produced *LHV* of about 3.05 MJ Nm^{-3} for air as a gasification agent in a downdraft gasifier. The syngas energy content from the studies [49,50] is lower than those reached in this work. Nevertheless, the *LHV* was poor when compared with other reports indicating values between 4.0 and 5.6 MJ Nm^{-3} for downdraft gasifiers and 3.7–5.1 MJ Nm^{-3} for (bottom lit) updraft operation [10,11]. Hence, strategies such as improving the insulation layer, implementing continuous feeding, and adding other gasification agents in the TLUD gasifier could enhance the *LHV* of the syngas.

In this study, the average equivalence ratio (Φ) varied from 0.30 (± 7.6%) to 0.34 (± 3.2%) due to diverse experimental conditions tested [38]. Here, the parenthesis terms represent the estimated relative uncertainty. This variation on Φ is the consequence of changes in the v_s values used in the experiments, the chemical composition of feedstocks, the natural variability of experiments, the nonuniformity distribution of the PKS-HVBC blends into the TLUD gasifier, and the wall heat transfer into the reactor. Thus, changes in v_s and in chemical composition affect the actual and stoichiometric air-fuel ratios, modifying the Φ values. Likewise, nonuniformity distributions into the bed produce variations on u_f, which enables estimating the actual air-fuel ratio, a variable necessary to calculate Φ. Nonuniform distributions occur due to the positions of PKS and HVBC particles in the bed, which have different bulk densities and randomly enter the gasifier, causing nonuniform feedstock consumption and probably producing channeling in the TLUD. On the other hand, the rise in the wall temperature in the gasifier alters the u_f behavior, increasing the feedstock consumption as a consequence of the enhancement o the heat transfer into the bed.

The slight difference in Φ obtained in the experiments did not cause high variations in the syngas composition; however, some trends are evident. Tests with 45 % wt of coal produced a high H_2 content, which was only about 0.7% higher than that one for tests with pure PKS and 9% higher than that obtained for 25% wt coal, which could indicate that at

Table 2
Average gas composition, higher (HHV_g) and lower (LHV_g) heating values of syngas derived from the co-gasification tests. The corresponding estimated uncertainty appears in parentheses.

Gas/parameter	Blend (Coal-Biomass, wt %-wt %)		
	45–55	25–75	0–100
H_2, vol %	6.77 (±0.070)	6.14 (±0.183)	6.72 (±0.048)
N_2, vol %	64.96 (±0.003)	64.07 (±0.620)	60.63 (±0.096)
CH_4, vol %	4.13 (±0.242)	3.52 (±0.095)	3.29 (±0.122)
CO, vol %	11.49 (±0.030)	12.02 (±0.239)	14.65 (±0.070)
CO_2, vol %	12.66 (±0.133)	14.26 (±0.292)	14.71 (±0.152)
Equivalence ratio, Φ	0.30 (±7.6%)	0.31 (±3.3%)	0.34 (±3.2%)
LHV_g, MJ Nm^{-3}	3.66 (±0.003)	3.44 (±0.003)	3.76 (±0.001)
HHV_g, MJ Nm^{-3}	3.97 (±0.003)	3.71 (±0.003)	4.02 (±0.001)

specific coal percentage, the H_2 production would reach a maximum value. This trend in the H_2 content was similar to that observed by Jeong et al. [51], who reported a reduction of this gas for tests with pure biomass compared to pure coal gasification. Therefore, future works in our TLUD gasifier could explore a higher coal percentage to observe its influence on the H_2 content.

On the other hand, the CO content was lower for tests with higher percentages of coal, a trend also observed by Mallick et al. [52] and Jeong et al. [51], who co-gasified coal and biomass in a fluidized bed using air as the gasification agent. Likewise, the CO_2 increased as the biomass percentage increased, reaching a maximum of 14.71% vol, with tests for pure biomass. Patel et al. [53] also observed an increase in the CO_2 content as the biomass share increased in the co-gasification of lignite and waste wood in a downdraft gasifier using air as the gasification agent. Regarding the CH_4 content, this gas was higher for tests with high coal percentages, being 4.13, 3.52, and 3.29% vol, for MP_c values of 45%, 25%, and 0% wt, respectively. However, these findings do not support the trend reported by Mallick et al. [52], who observed higher CH_4 contents for pure biomass tests. On the contrary, Patel et al. [53] did not observe significant changes in the CH_4 production during their tests with biomass and coal, resulting in a consistent level of this gas throughout their study.

Finally, the carbon conversion efficiency (*CCE*), defined as the percentage volume ratio of the carbonaceous gas compounds in the syngas regarding the solid carbon contained in feedstock [54], measures the conversion of carbon of biomass and coal in products such as CO, CO_2, and CH_4. Syngas from pure biomass featured a higher *CCE* increase, ranging from 64, 82, and 84%, for the low, medium, and high v_s values, respectively, representing an increase of 22% for this variable when v_s changes from minimum to maximum. Similarly, tests with 25% and 45% wt coal showed an augment in *CCE* of 20% and 12%, respectively. These results are consistent with the syngas composition depicted in Table 2.

3.3. Natural gas-syngas interchangeability through Delbourg's method

Table 3 shows the reference natural gases used in this study. These gases present diverse chemical compositions and different energy content. For example, NG_1 has a lower CH_4 value than NG_2 and NG_3, but it has a high C_2H_6 value for these gases, reaching 98% and 13% higher than NG_2 and NG_3, respectively. Likewise, NG_2 has more CH_4 content than NG_1 and NG_2, but it contains a lower *LHV* when compared with NG_1 and NG_3, which have a similar *LHV*. On the other hand, according to the online calculator developed by Cummins [42], the methane number for these gases was higher for NG_2, followed by NG_1 and NG_3, respectively.

Fig. 2 shows the Delbourg diagram for syngas obtained from 25 to 45 wt % of coal blended with NGs evaluated in this study. To evaluate their interchangeability, the syngas share in the blends changed in the range of 10–20 vol %. The Delbourg's approach defines a boundary, which

Table 3
Chemical composition, lower heating value (*LHV*), and methane number (*MN*) of natural gas types evaluated in this study. Chemical composition adapted from Ref. [55].

Gas/parameter	Natural gas type		
	NG_1	NG_2	NG_3
H_2, vol %	0.00	0.00	0.00
N_2, vol %	0.9	1.44	0.54
CH_4, vol %	81.93	98.14	83.78
CO, vol %	0.00	0.00	0.00
CO_2, vol %	3.18	0.11	1.94
C_2H_6 vol %	11.62	0.25	10.11
C_3H_8 vol %	1.92	0.06	3.63
C_4H_{10} vol %	0.45	0.01	0.00
LHV, MJ Nm^{-3}	39.3	35.5	40.0
MN	73.7	98.6	72.6

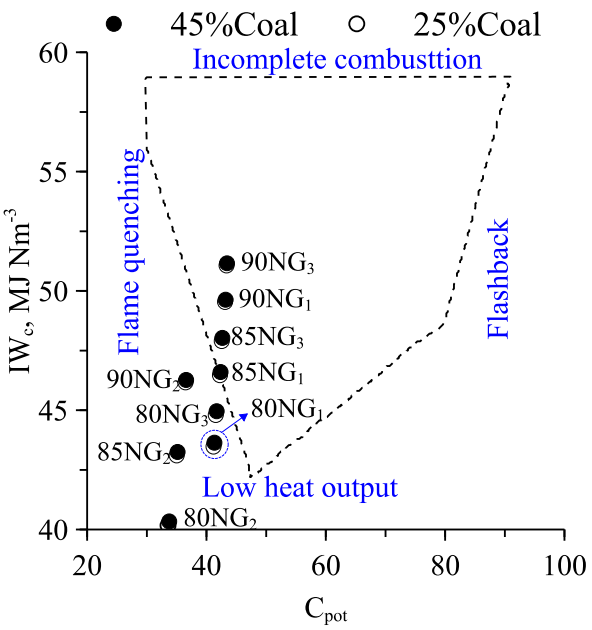

Fig. 2. Interchangeability analysis of syngas-NG blends for different coal percentages. The numerical value accompanying NG represents the volumetric percentage of this gas in the syngas-NG blends. Thus, 80NG is a blend with 80 vol % of NG and 20 vol % of syngas (20-80NG).

determines a desirable operating zone, using IW_c and C_{pot} as the ordinate and the abscissa, respectively. In the Delbourg diagram, the boundary region defined by the black dashed line indicates a proper operation in burners working at atmospheric pressure. Blends on the left side of the boundary undergo flame quenching associated with lifting flame troubles, while the flame tends to expire for those on the right side, tending to produce flashbacks. Similarly, blends on the lower part of the boundary combust with excessive air, reducing the heat supplied by the burner. Conversely, the process undergoes partial combustion if the blends fall on the upper part of the diagram [56].

As shown in Fig. 2, syngas-NG blends with $80NG_1$ fall outside the operating region, indicating no interchangeability. Moreover, all syngas-NG_2 mixtures in Fig. 2 are not interchangeable without burner modifications. In all cases shown in Fig. 2, a maximum of 15 vol % of syngas could operate with NG_3 in atmospheric burners. In addition, 10 vol % of syngas would work with NG_1 for all cases. Cases with 15 vol % of syngas blended with NG_1 are on the dashed black line boundary, representing potential operating issues in the burner. Hence, the syngas-NG blends outside the boundary region are not interchangeable without modifying the burner [56].

Table 4 shows the interchangeability results for syngas-NG blends, with syngas derived from pure biomass. Table 4 indicates that blends with 15 vol % syngas and 85 vol % NG_3 are interchangeable, as shown in Fig. 2. The same result applies to 10 vol % syngas and 90 vol % NG_1, while all mixtures with NG_2 are not interchangeable, according to Delbourg's method.

Results show that a maximum of 15 vol % of syngas blended with NG_3 shows favorable interchangeability. A higher LHV_g of syngas could enable an increase in the syngas share; therefore, future works should focus on improving LHV_g. For example, using different gasification agents in the TLUD gasifier, such as oxygen-enriched air, air preheating, or pure oxygen, are strategies that could enhance the energy content of the syngas [38]. For example, Sharma et al. [57] observed an increase in the LHV_g when adding steam into the reduction zone of a downdraft gasifier. Diverse authors reported an increase in the LHV_g of syngas for gasification agents other than pure air [58,59].

Table 4
Gas interchangeability results for syngas-natural gas blends, syngas from 100% biomass. Chemical composition in %Vol. The estimated uncertainty appears in parentheses for IW_c and C_{pot}.

Syngas-NG blends, vol %-vol %	CH_4	C_2H_6	C_3H_8	C_4H_{10}	CO	H_2	N_2	CO_2	IW_c, MJ Nm^{-3}	C_{pot}	Interchangeable
20-80NG_1	66.20	9.30	1.54	0.36	2.93	1.34	12.85	5.49	43.53 (±0.0008)	41.71 (±0.5907)	No
15-85NG_1	70.13	9.88	1.63	0.38	2.20	1.01	9.86	4.91	46.52 (±0.0008)	42.66 (±0.3039)	No
10-90NG_1	74.07	10.46	1.73	0.41	1.47	0.67	6.87	4.33	49.57 (±0.0008)	43.39 (±0.6740)	Yes
20-80NG_2	79.16	0.20	0.05	0.01	2.93	1.34	13.28	3.03	40.23 (±0.0009)	34.15 (±0.8304)	No
15-85NG_2	83.91	0.21	0.05	0.01	2.20	1.01	10.32	2.30	43.16 (±0.0009)	35.43 (±0.9324)	No
10-90NG_2	88.65	0.22	0.05	0.01	1.46	0.67	7.36	1.57	46.20 (±0.0010)	36.28 (±1.0550)	No
20-80NG_3	67.68	8.09	2.90	–	2.93	1.34	12.56	4.49	44.85 (±0.0008)	42.09 (±0.6081)	No
15-85NG_3	71.71	8.59	3.09	–	2.20	1.01	9.55	3.86	47.94 (±0.0008)	42.96 (±0.6508)	Yes
10-90NG_3	75.73	9.10	3.27	–	1.47	0.67	6.55	3.22	51.10 (±0.0008)	43.63 (±0.7004)	Yes

3.3.1. *Combustion of syngas-natural gas blends*

This section presents the results of the combustion of syngas-NG blends at different Φ values. The study estimates the flue gas composition and T_{adb} through a thermodynamic analysis via Chemkin Pro®, using the solver "Chemical and Phase Equilibrium Calculation." The oxidizer was dry air (21% O_2, 79% N_2, vol %) at 298 K and 101.325 kPa. In addition, this section also shows S_L estimations, implementing the premix code of the same software for the assessed syngas-NG blends using a procedure similar to that reported in Ref. [60]. Section S5 in the supplementary material provides further information on the S_L estimation.

Fig. 3a shows the flue gas composition of the syngas-NG_3 mixtures changing Φ from 0.6 to 1.4. Adding 15 vol % of syngas causes only minor changes in the combustion gases. Additionally, H_2 and CO contents are evident when Φ ranges from 0.6 to 1.0, which is a consequence of incomplete combustion. Therefore, slight variations in H_2 and CO for the original fuel (NG_3), compared with those obtained with Syngas-NG_3 blends, are the first indication of the proper operation of these blends in atmospheric burners. H_2 and CO have a wide range of flammability that represents a drawback for fire safety, but are advantages regarding flame stability and emission reduction due to H_2 content [17]. However, as Φ increases, more oxygen is available for oxidation, reducing H_2 and CO concentrations.

On the other hand, CO_2 was higher for syngas-NG_3 blends, which could be associated with higher content of CO_2 in syngas from pure biomass. Note that for Φ values higher than 1.0, CO_2 behavior is similar for both fuels. Conversely, H_2O has similar concentrations for Φ between 0.6 and 0.8, but for higher values of Φ, H_2O is lower for syngas-NG_3 blends. Due to the neutral carbon feature of biomass, syngas-NG_3 blends could represent an attractive option to supply thermal energy while contributing to reducing CO_2 emissions. Finally, NO concentrations do not show significant changes in the combustion process of the evaluated conditions.

Fig. 3b shows T_{adb} and S_L for different Φ values of NG_3 and syngas-NG_3 blends. Results indicate that for Φ values lower than 0.9, T_{adb} does not undergo significant variations. However, for Φ values higher than 0.9, NG_3 reaches higher temperatures than those obtained for syngas-NG_3 blends. Nevertheless, for the Φ values evaluated here, the temperature difference was between 8 and 19 K, which would not result in significant changes in burner performance. On the other hand, those industrial processes that do not accept higher variations in temperature could compensate for the required value *via* air preheating, which represents an alternative route to using the syngas-NG_3 blends, ensuring the necessary temperature. However, auto-ignition temperatures of the fuel gases restrict maximum preheating temperatures. For example, H_2 and CO have auto-ignition temperatures of about 773 K and 882 K, respectively [1]. Thus, this value will restrict air preheating temperature to 773 K for H_2, representing the upper limit.

Fig. 3b also shows the S_L behavior for different Φ values. Using syngas-NG blends affects laminar flame velocity in combustion devices because of the changes in gas composition. The laminar flame velocity is representative of the combustion process, revealing information associated with the reactivity, diffusivity, and exothermicity of a fuel burning in a combustion device [61]. Mixtures of 15 vol % syngas derived from 100% biomass blended with NG_3 only cause minor changes in S_L. The higher difference in this parameter occurs for Φ values between 1.0 and 1.3, with S_L around 3.8% lower than that for pure NG_3 using the USC-Mech II reaction mechanism [62]. Hernández et al. [63] reported that H_2 in the syngas increased the S_L value in an atmospheric burner operating with syngas and natural gas mixtures. Hydrogen could reach S_L values five times higher than CH_4 [64]. Albeit the syngas adds H_2 to syngas-NG_3 blends, its relatively low share in these blends does not cause a significant influence on laminar flame velocity because other gases such as N_2 and CO_2 reduce the thermal diffusivity and the flame

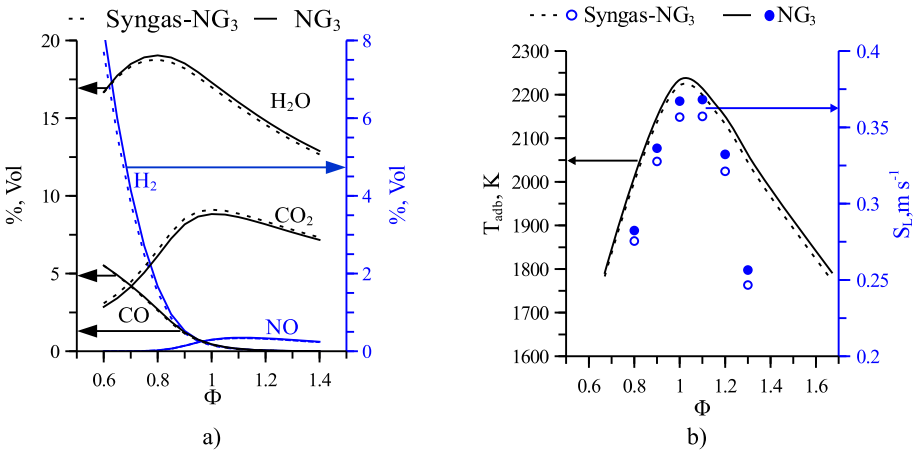

Fig. 3. a) Flue gas compositions for syngas-NG_3 blends for different values of the equivalence ratio (Φ), b) Adiabatic flame temperatures (black dashed and continued lines) and laminar flame velocity (S_L, blue symbols) for syngas-NG_3 blends using different Φ values.

temperature of syngas-NG_3 blends combustion [61], thus restricting the increase on S_L. The slight differences between S_L values for pure NG_3 and those for syngas-natural gas blends ensure that, under the same operating conditions, combustion in the burner remains stable, i.e., the burner could not present instability problems such as lift-off, blow-off, quenching, and flashback, among others. These are promising results for the interchangeability of syngas-NG_3 blends, according to Delbourg's method.

3.4. Combustion potential, corrected Wobbe index, and methane number for syngas, natural gas, and their blends

We incorporated the *MN* of syngas, NG, syngas-NG blends, and complementary gases in the Delbourg diagram to assess the trends followed by these gases regarding IW_c, C_{pot}, and *MN*. Fig. 4 plots the IW_c and the *MN* of the gases as a function of C_{pot}. This figure, also included gases from chemical processes and typical natural gases studied by Leiker et al. [41], to gain further insight. Table 5 shows the methane number for syngas from pure biomass, natural gases, and syngas-NG blends that were interchangeable, according to Table 4.

According to Fig. 4, although NG_2 is interchangeable with NG_1, NG_3, and syngas-NG fuel blends, it has a higher methane number, which correlates with its combustion performance in applications such as ICEs and GTs. Fig. 4 also shows the strong correlation between C_{pot} and *MN* for different fuels. Thus, fuel gas with higher knock-resistance, such as syngas from pure biomass, presents a lower C_{pot}, whereas lower knock-resistance fuels, such as H_2 and C_2H_4, have a higher C_{pot}. It is interesting to note how fuels with different compositions follow this trend. The dilution of fuels of high *MN* using inert gases such as nitrogen and carbon dioxide and the effect of hydrogen concentration in fuel gases with low *MN*, explain this trend. Specifically, inert gases reduce the mole fraction of active components such as hydrogen, methane, and hydrocarbons, thus reducing C_{pot}. Furthermore, other studies have observed that an increase in the CO content of the fuel gas also increases its knock limit [65,66].

Fig. 4 and Table 4 show that, for NG_1 and NG_3, the 15-85NG_3, 10-90NG_3, and 10-90NG_1 blends, for syngas from pure biomass, only present slight variations in *MN*, i.e., operating with NG_1 and NG_3, the addition of syngas in the above percentages would not affect the operating conditions in ICEs. The higher variations in *MN* occur for 15-85NG_3, which is 5.8% higher than that for NG_3, while the 10-90NG_1 blend has a methane number 3.2% higher than NG_1's. On the other hand, comparing *MNs* for the 15-85NG_3 and 10-90NG_1 blends, regarding NG_2, shows the differences reaching numbers around 16%, indicating

Table 5
Methane number for syngas, natural gases, and syngas-NG blends evaluated in this research. Syngas corresponds to those obtained from 100% biomass. The estimated uncertainty appears in parentheses.

Gas/Syngas-NG blends	*MN*
NG_1	75.4
NG_2	92.3
NG_3	73.7
100% Biomass	160 (±30.9)
10-90NG_3, vol %-vol %	76.5
15-85NG_3, vol %-vol %	78.2
10-90NG_1, vol %-vol %	77.9

that these mixtures could present unusual combustion in ICEs. This trend occurs because of the high methane content of NG_2, as shown in Table 3. This result is also evident in Fig. 4, which shows the proximity of *MN* values for CH_4 and NG_2, the latter being 7.7% lower than the former. The red dashed lines in Fig. 4 indicate the regions for gases of the first and second family, tagged as Blasts Furnace Gas-Coke Gas and Natural Gases, respectively.

We developed a further assessment between these variables and S_L for selected gases to uncover more trends with IW_c, C_{pot}, and *MN*. Section S6 in the supplementary material shows a complete description of the main results. Moreover, Figure S6.1 shows the Delbourg diagram using S_L as a secondary axis for the studied fuels. This Figure illustrates that S_L calculated values are similar for gases of the second family [16]. The mean laminar flame velocity of these fuels amounts to 0.3575 m s^{-1}, with the maximum and minimum values being 0.3649 and 0.3514 m s^{-1}. Therefore, from an interchangeability perspective, the methane number for the gases evaluated in this research is the most significant variable for the second family of gases. Hence, attention should be paid to the difference in their *MNs*, as was described in this section.

4. Perspectives

The abovementioned sections described the characteristics of syngas produced from the co-gasification of coal and biomass in a TLUD gasifier. This study assessed the interchangeability of NGs with syngas-NG blends in atmospheric burners and high-pressure combustion devices. A maximum share of 15 vol % of syngas enabled the formation of blends with natural gas without altering the operating conditions in atmospheric burners. A higher syngas share could be reached as the *LHV* of the syngas is enhanced. Thus, diverse strategies such as changing the

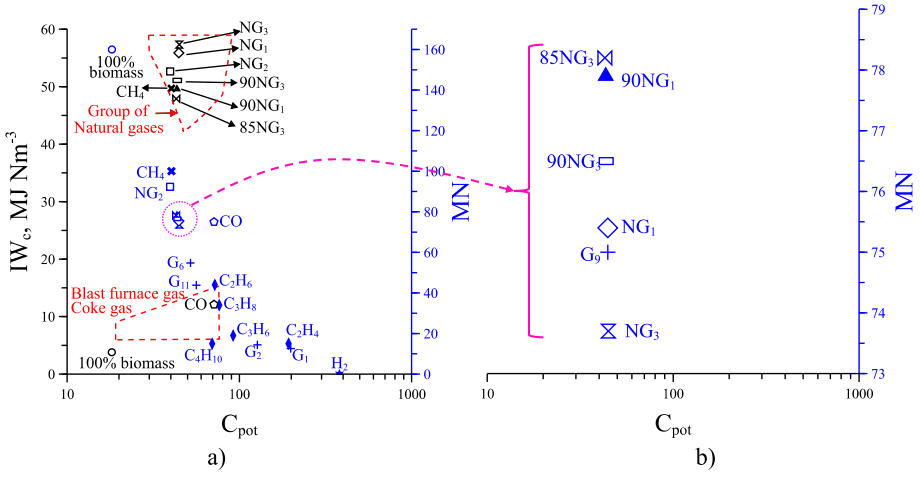

Fig. 4. a) Methane number behavior for syngas, NG, syngas-NG blends, and complementary fuel gases, represented in the Delbourg diagram. b) Visual enhancement of magenta dotted line. Points 85NG_3, 90NG_3, and 90NG_1 are syngas-NG blends representing 15-85NG_3, 10-90NG_3, and 10-90NG_1, respectively. The chemical composition of gases G_1, G_2, G_6, G_9, and G_{11} appears in Table S4.1 in the supplementary material [41].

reducing agents for gasification are feasible to improve syngas quality. For example, steam or pure oxygen combined with air can increase the energy content of the syngas as compared to air [57,59,67]. In terms of an interchangeability analysis, an improved syngas energy content implies a high percentage of syngas in the blends with natural gas. However, additional combustion properties that influence combustion stability should be evaluated. Among others, it is necessary to include estimations of flue gases, flame temperature, laminar flame velocity, NO_x formation, and heat transfer to determine the maximum share of syngas and their effects on the operating conditions of combustion devices.

Fuel gases in fixed bed gasification systems mainly consist of H_2, CO, and CH_4, with the latter in concentrations lower than 5 vol % on a dry basis [67,68], while H_2 and CO have higher concentrations. Nevertheless, gases such as N_2 and CO_2 are also present in gasification systems, which cannot participate in combustion reactions, but absorb part of the energy released in the combustion process. In addition, the N_2 and CO_2 from syngas and those gases released in the combustion reaction could affect the radiation properties of the appraised thermal application because the gas emissivity changes, also modifying the heat transfer distribution in the process. Besides this, the addition of CO and H_2 from the syngas to the natural gas will affect the flame temperature and laminar flame velocity of the combustion process, which represent additional challenges that must be controlled to ensure the stability of the process. For example, H_2 has S_L values about five times higher than CH_4, while CO could reach S_L values similar to, or slightly higher than, CH_4 [64]. On the other hand, the adiabatic flame temperature of H_2 and CO could be 8% higher than that of CH_4 when air is the oxidizer [69], implying that the equivalence ratio could require modifications to ensure the proper temperature in the combustion process while ensuring complete fuel conversion.

In ICEs, syngas can be used as primary or secondary fuel for transportation or power generation applications. Some studies report the use of syngas in compression ignition engines in which diesel serves as a pilot fuel to ignite the mixtures, whereas others describe syngas inclusion in dual-fuel engines to replace the higher diesel share [70]. Regardless of use, challenges associated with the injection timing and the air displacement in the combustion chamber, which affects the engine volumetric efficiency, limit the maximum share of syngas used. In spark ignition engines, syngas could replace natural gas or gasoline. However, engine performance will be affected because the low density of the syngas reduces the engine volumetric efficiency. Increasing the compression ratio (avoiding the knock effect), using direct fuel injection, and implementing superchargers or turbochargers could improve efficiency when syngas is used as fuel in ICEs. Albeit of the above-mentioned challenges or drawbacks, the inclusion of syngas could reduce pollutant emissions [66], representing a significant advantage compared to conventional systems [70]. In addition, high H_2 content in syngas could increase operating range and thermal efficiency in ICEs operating in dual fuel mode, but the NO_x will also increase [71].

5. Conclusions

This study assessed the natural gas interchangeability with syngas derived from the co-gasification of PKS-HVBC. Different syngas percentages with typical natural gases used in Colombia and the flue gas compositions at various Φ values allowed for assessing the potential of syngas as an alternative fuel for thermal applications. Delbourg's approach and *MN* estimation were used as complementary methods to evaluate the syngas-NG interchangeability in atmospheric natural gas burners and high-pressure combustion applications. Results showed that 15 vol % of syngas derived from co-gasification of PKS-HVBC could operate with NG_3 in natural gas burners without affecting their operating conditions. Likewise, *MN* for blends with 15 vol % of syngas was only 5.8% higher than that of natural gas, indicating proper operation of this blend in high-pressure combustion applications.

The inclusion of *MN* as a new axis in the Delbourg diagram illustrates the trends followed by this parameter for the fuel gases evaluated. Results evidence that *MN* presents a stronger correlation with C_{pot} for different gaseous fuels. Syngas from pure biomass showed the highest *MN* of the evaluated fuels and the lowest C_{pot}. Thus, as *MN* decreases, the C_{pot} increases, revealing the influence of high hydrogen content of fuel gases with low *MN*. In addition, the dilution of gaseous fuels with high *MN* using inert gases such as N_2 and CO_2 can also explain the observed trends.

Slight differences in the flue gas compositions, T_{adb}, and S_L, give insights into the proper operation of syngas-NG_3 blends as a substitute fuel for pure NG_3. Results showed that CO_2 and H_2O for syngas-NG_3 mixtures were 3.3% higher and 4.3% lower, respectively than for NG_3. In addition, for the Φ assessed values, T_{adb} decreased between 8 and 19 K for syngas-NG_3 blends as compared to NG_3. Similarly, S_L showed minor changes in their behavior for the studied Φ ranges. The slight variations in the variables above allowed for validation of the interchangeability results obtained from Delbourg's method and *MN*, for syngas-NG_3 mixtures.

A greater attention to syngas studies for industrial applications is recommended due to the pressing need to incorporate higher proportions of alternative energy into our energy systems. Dual fuel combustion in ICEs and interchangeability analysis are two promising research areas for further exploring the integration of syngas in thermal applications.

Credit author statement

Daniel A. Quintero-Coronel: writing original draft, investigation, formal analysis**. Adalberto Salazar**: Methodology, validation, formal analysis**. Oscar R. Pupo-Roncallo**: Formal analysis, writing - review & editing**. Antonio Bula**: Formal analysis, resources, writing - review & editing**. Lesme Corredor**: Conceptualization, funding acquisition, project administration**. German Amador**: Methodology, validation, formal analysis, writing - review & editing**. Arturo Gonzalez-Quiroga**: writing - review & editing, conceptualization, supervision.

Declaration of competing interest

The authors declare that they have no known competing financial interests or personal relationships that could have appeared to influence the work reported in this paper.

Data availability

Data will be made available on request.

Acknowledgements

MINCIENCIAS supported this work through the Ph.D. National Scholarship Becas Bicentenario 2019 Contract UN-OJ-2020-47414. The authors would like to acknowledge the financial support granted by the Agencia Nacional de Investigación y Desarrollo (ANID) of the Chilean government through the project Fondecyt Iniciación No 11190447, the dirección de postgrados y programas of the Universidad Tecnica Federico Santa Maria.

Appendix A. Supplementary data

Supplementary data to this article can be found online at https://doi.org/10.1016/j.energy.2023.127551.

References

[1] Gómez HO, Calleja MC, Fernández LA, Kiedrzyńska A, Lewtak R. Application of the CFD simulation to the evaluation of natural gas replacement by syngas in burners

of the ceramic sector. Energy 2019;185:15–27. https://doi.org/10.1016/j.energy.2019.06.064.
[2] Afkhami B, Akbarian B, Beheshti N, Kakaee AH, Shabani B. Energy consumption assessment in a cement production plant. Sustain Energy Technol Assessments 2015;10:84–9. https://doi.org/10.1016/j.seta.2015.03.003.
[3] Herzler J, Herbst J, Kick T, Naumann C, Braun-Unkhoff M, Riedel U. Alternative fuels based on biomass: an investigation of combustion properties of product gases. J Eng Gas Turbines Power 2013;135(3):1–9. https://doi.org/10.1115/1.4007817.
[4] Ali DA, Gadalla MA, Abdelaziz OY, Hulteberg CP, Ashour FH. Co-gasification of coal and biomass wastes in an entrained flow gasifier: modelling, simulation and integration opportunities. J Nat Gas Sci Eng 2017;37:126–37. https://doi.org/10.1016/j.jngse.2016.11.044.
[5] Jóźwiak P, Hercog J, Kiedrzyńska A, Badyda K. CFD analysis of natural gas substitution with syngas in the industrial furnaces. Energy 2019;179:593–602. https://doi.org/10.1016/j.energy.2019.04.179.
[6] ISO. In: ISO 13686:2013 Natural gas — Quality designation, vol. 2013; 2013. p. 48 [Online]. Available: https://www.iso.org/obp/ui/#iso:std:iso:13686:ed-2:v1:en:sec:A.
[7] Kamble AD, Saxena VK, Chavan PD, Mendhe VA. Co-gasification of coal and biomass an emerging clean energy technology: status and prospects of development in Indian context. Int J Min Sci Technol 2019;29(2):171–86. https://doi.org/10.1016/j.ijmst.2018.03.011.
[8] Tinaut FV, Melgar A, Pérez JF, Horrillo A. Effect of biomass particle size and air superficial velocity on the gasification process in a downdraft fixed bed gasifier. An experimental and modelling study. Fuel Process Technol 2008;89(11):1076–89. https://doi.org/10.1016/j.fuproc.2008.04.010.
[9] Kirch T, Medwell PR, Birzer CH, van Eyk PJ. Small-scale autothermal thermochemical conversion of multiple solid biomass feedstock. Renew Energy 2020;149:1261–70. https://doi.org/10.1016/j.renene.2019.10.120.
[10] Saravanakumar A, Haridasan TM, Reed TB, Bai RK. Experimental investigation and modelling study of long stick wood gasification in a top lit updraft fixed bed gasifier. Fuel 2007;86(17–18):2846–56. https://doi.org/10.1016/j.fuel.2007.03.028.
[11] Couto N, Rouboa A, Silva V, Monteiro E, Bouziane K. Influence of the biomass gasification processes on the final composition of syngas. Energy Proc 2013;36:596–606. https://doi.org/10.1016/j.egypro.2013.07.068.
[12] Kiedrzyńska A, Lewtak R, Świątkowski B, Jóźwiak P, Hercog J, Badyda K. Numerical study of natural gas and low-calorific syngas co-firing in a pilot scale burner. Energy 2020;211. https://doi.org/10.1016/j.energy.2020.118552.
[13] Honus S, Kumagai S, Němček O, Yoshioka T. Replacing conventional fuels in USA, Europe, and UK with plastic pyrolysis gases – Part I: experiments and graphical interchangeability methods. Energy Convers Manag 2016;126:1118–27. https://doi.org/10.1016/j.enconman.2016.08.055.
[14] Afanador JMO, Alvarado LV. Informe: estado del arte intercambiabilidad a nivel internacional. Bucaramanga. 2016. p. 66 [Online]. Available: www.polygon.com.co.
[15] Honus S, Kumagai S, Yoshioka T. Replacing conventional fuels in USA, Europe, and UK with plastic pyrolysis gases – Part II: multi-index interchangeability methods. Energy Convers Manag 2016;126:1128–45. https://doi.org/10.1016/j.enconman.2016.08.054.
[16] Flórez-Orrego D. Métodos para el estudio de la intercambiabilidad de una mezcla de Gas Natural y Gas Natural-Syngas en quemadores de premezcla de régimen laminar: un artículo de revisión. 2011. https://doi.org/10.13140/RG.2.2.32284.03202.
[17] Raghavan V. Burners for gaseous fuels. In: Combustion technology. John Wiley & Sons, Ltd; 2016. p. 105–38. https://doi.org/10.1002/9781119241775.ch4.
[18] Munajat NF, Erlich C, Fakhrai R, Fransson TH. Influence of water vapour and tar compound on laminar flame speed of gasified biomass gas. Appl Energy 2012;98:114–21. https://doi.org/10.1016/j.apenergy.2012.03.010.
[19] Yan B, et al. Experimental and modeling study of laminar burning velocity of biomass derived gases/air mixtures. Int J Hydrogen Energy 2011;36(5):3769–77. https://doi.org/10.1016/j.ijhydene.2010.12.015.
[20] Richter S, Ermel J, Kick T, Braun-Unkhoff M, Naumann C, Riedel U. The influence of diluent gases on combustion properties of natural gas: a combined experimental and modeling study. J Eng Gas Turbines Power 2016;138(10):1–9. https://doi.org/10.1115/1.4033160.
[21] Papafilippou N, Chishty MA, Gebart R. On the flame shape in a premixed swirl stabilised burner and its dependence on the laminar flame speed. Flow, Turbul Combust 2022;108(2):461–87. https://doi.org/10.1007/s10494-021-00279-6.
[22] Andrade RV, et al. Assessment of laminar flame velocity of producer gas from biomass gasification using the Bunsen burner method. Int J Hydrogen Energy 2020;45(20):11559–68. https://doi.org/10.1016/j.ijhydene.2020.02.082.
[23] Diaz GJA, Martinez LMC, Montoya JPG, Olsen DB. Methane number measurements of hydrogen/carbon monoxide mixtures diluted with carbon dioxide for syngas spark ignited internal combustion engine applications. Fuel 2019;236:535–43. https://doi.org/10.1016/j.fuel.2018.09.032. August 2018.
[24] Gupta SK, Mittal M. Predicting the methane number of gaseous fuels using an artificial neural network. Biofuels 2021;12(10):1191–8. https://doi.org/10.1080/17597269.2019.1600455.
[25] Malenshek M, Olsen DB. Methane number testing of alternative gaseous fuels. Fuel 2009;88(4):650–6. https://doi.org/10.1016/j.fuel.2008.08.020.
[26] Wise DM, Olsen DB, Kim M. Characterization of Methane Number for Producer Gas Blends 2013;2. https://doi.org/10.1115/ICEF2013-19221.
[27] Diderich G, Scherm P. Requirements on the quality of natural gas. 2017-11–9 Eur. Assoc. Intern. Combust. Engine Manuf. 2017 [Online]. Available: https://www.euromot.eu/wp-content/uploads/2018/02/EUROMOT-Position-Gas-Quality-2017-11-09-.pdf.
[28] Zardoya AR, Lucena IL, Bengoetxea IO, Orosa JA. Research on an internal combustion engine with an injected pre-chamber to operate with low methane number fuels for future gas flaring reduction. Energy 2022;253. https://doi.org/10.1016/j.energy.2022.124096.
[29] Caligiuri C, et al. Complementing syngas with natural gas in spark ignition engines for power production: effects on emissions and combustion. Energies 2021;14(12). https://doi.org/10.3390/en14123688.
[30] Rabello de Castro R, Brequigny P, Mounaïm-Rousselle C. A multiparameter investigation of syngas/diesel dual-fuel engine performance and emissions with various syngas compositions. Fuel 2022;318(x):123736. https://doi.org/10.1016/j.fuel.2022.123736.
[31] Kohn MP, Lee J, Basinger ML, Castaldi MJ. Performance of an internal combustion engine operating on landfill gas and the effect of syngas addition. Ind Eng Chem Res 2011;50(6):3570–9. https://doi.org/10.1021/ie101937s.
[32] Ji C, Dai X, Wang S, Liang C, Ju B, Liu X. Experimental study on combustion and emissions performance of a hybrid syngas-gasoline engine. Int J Hydrogen Energy 2013;38(25):11169–73. https://doi.org/10.1016/j.ijhydene.2013.02.101.
[33] Zarenezhad Ashkezari A. Numerical analysis of performance and emissions behavior of a bi-fuel engine with compressed natural gas enriched with hydrogen using variable compression ratio strategy. Int J Hydrogen Energy 2022;47(19):10762–76. https://doi.org/10.1016/j.ijhydene.2022.01.129.
[34] Nadaleti WC, Przybyla G. SI engine assessment using biogas, natural gas and syngas with different content of hydrogen for application in Brazilian rice industries: efficiency and pollutant emissions. Int J Hydrogen Energy 2018;43(21):10141–54. https://doi.org/10.1016/j.ijhydene.2018.04.073.
[35] Olanrewaju FO, Li H, Aslam Z, Hammerton J, Lovett JC. Analysis of the effect of syngas substitution of diesel on the Heat Release Rate and combustion behaviour of Diesel-Syngas dual fuel engine. Fuel December 2021;312. https://doi.org/10.1016/j.fuel.2021.122842. 2022.
[36] Krishnamoorthi M, Sreedhara S, Prakash Duvvuri P. Experimental, numerical and exergy analyses of a dual fuel combustion engine fuelled with syngas and biodiesel/diesel blends. Appl Energy 2020;263. https://doi.org/10.1016/j.apenergy.2020.114643. February.
[37] Lenis YA, Agudelo AF, Pérez JF. Analysis of statistical repeatability of a fixed bed downdraft biomass gasification facility. Appl Therm Eng 2013;51(1–2):1006–16. https://doi.org/10.1016/j.applthermaleng.2012.09.046.
[38] Quintero-Coronel DA, Lenis-Rodas YA, Corredor L, Perreault P, Bula A, Gonzalez-Quiroga A. Co-gasification of biomass and coal in a top-lit updraft fixed bed gasifier: syngas composition and its interchangeability with natural gas for combustion applications. Fuel October 2021;316:123394. https://doi.org/10.1016/j.fuel.2022.123394. 2022.
[39] Waldheim T, Nilsson L. Heating value of gases from biomass gasification. Task 20 - Therm. Gasif. Biomass, no. May. IEA Bioenergy Agreement; 2001. p. 61 [Online]. Available: http://www.ieatask33.org/app/webroot/files/file/publications/HeatingValue.pdf.
[40] Xiang L, Theotokatos G, Ding Y. Investigation on gaseous fuels interchangeability with an extended zero-dimensional engine model. Energy Convers Manag 2019;183:500–14. https://doi.org/10.1016/j.enconman.2019.01.013.
[41] Leiker M, Christoph K, Rankl M, Catellier W, Pfeifer U. Evaluation of antiknocking property of gaseous fuels by means of methane number and its practical application to gas engines. ASME; 1972.
[42] Wärtsilä. Wärtsilä methane number calculator. 2020. accessed Sep. 29, 2022, https://www.wartsila.com/marine/products/gas-solutions/methane-number-calculator.
[43] Arunachalam A, Olsen DB. Experimental evaluation of knock characteristics of producer gas. Biomass Bioenergy 2012;37:169–76. https://doi.org/10.1016/j.biombioe.2011.12.016.
[44] Bell Stephanie, Measurement Good Practice Guide No. 11-A beginner's guide to uncertainty of measurement. 2013 [Online]. Available: https://www.npl.co.uk/gpgs/beginners-guide-measurement-uncertainty-gpg11.
[45] Verdeza-Villalobos A, Lenis-Rodas YA, Bula-Silvera AJ, Mendoza-Fandiño JM, Gómez-Vásquez RD. Performance analysis of a commercial fixed bed downdraft gasifier using palm kernel shells. CTyF - Ciencia, Tecnol. y Futur. 2019;9(2):79–88. https://doi.org/10.29047/01225383.181.
[46] Zapata RB, Bayer JFP, Jiménez CS. Carbones colombianos : clasificación y caracterización termoquímica para aplicaciones energéticas Colombian coals : classification and thermochemical characterization for energy applications Carvões colombianos : classificação e caracterização para aplica. Rev. ION 2014;27(2):43–54.
[47] Gaur S, Reed TBTB. An atlas of thermal data for biomass and other fuels," *Nrel.* Golden, CO (United States): National Renewable Energy Lab.; 1995. p. 1–189.
[48] Mason DM, Gandhi KN. Formulas for calculating the calorific value of coal and coal chars: development, tests, and uses. Fuel Process Technol 1983;7(1):11–22. https://doi.org/10.1016/0378-3820(83)90022-X.
[49] Thiagarajan J, Srividhya PK, Balasubramanian P. Thermochemical behaviors and co-gasification kinetics of palm kernel shells with bituminous coal. Biomass Convers. Biorefinery 2020;10(3):697–706. https://doi.org/10.1007/s13399-019-00450-0.
[50] Thengane SK, Gupta A, Mahajani SM. Co-gasification of high ash biomass and high ash coal in downdraft gasifier. Bioresour Technol 2019;273:159–68. https://doi.org/10.1016/j.biortech.2018.11.007. November.
[51] Jeong YS, Choi YK, Park KB, Kim JS. Air co-gasification of coal and dried sewage sludge in a two-stage gasifier: effect of blending ratio on the producer gas

composition and tar removal. Energy 2019;185:708–16. https://doi.org/10.1016/j.energy.2019.07.093.
[52] Mallick D, Mahanta P, Moholkar VS. Co–gasification of coal/biomass blends in 50 kWe circulating fluidized bed gasifier. J Energy Inst 2020;93(1):99–111. https://doi.org/10.1016/j.joei.2019.04.005.
[53] Patel VR, Patel D, Varia NS, Patel RN. Co-gasification of lignite and waste wood in a pilot-scale (10kWe) downdraft gasifier. Energy 2017;119:834–44. https://doi.org/10.1016/j.energy.2016.11.057.
[54] Mahapatro A, Mahanta P. Gasification studies of low-grade Indian coal and biomass in a lab-scale pressurized circulating fluidized bed. Renew Energy 2020;150:1151–9. https://doi.org/10.1016/j.renene.2019.10.038.
[55] Barreto O. Comparación del desempeño de varias calidades de gas natural y evaluación de viabilidad para el uso de biogás como combustible para vehículos que operan con GNCV. Universidad Nacional de Colombia; 2017 [Online]. Available: https://repositorio.unal.edu.co/handle/unal/59902%0Ahttps://tel.archives-ouvertes.fr/tel-01514176.
[56] Honus S, Juchelkova D, Campen A, Wiltowski T. Gaseous components from pyrolysis - characteristics, production and potential for energy utilization. J Anal Appl Pyrolysis 2014;106:1–8. https://doi.org/10.1016/j.jaap.2013.11.023.
[57] Sharma S, Sheth PN. Air-steam biomass gasification: experiments, modeling and simulation. Energy Convers Manag 2016;110:307–18. https://doi.org/10.1016/j.enconman.2015.12.030.
[58] Ngamchompoo W, Triratanasirichai K. Experimental investigation of high temperature air and steam biomass gasification in a fixed-bed downdraft gasifier. Energy Sources, Part A Recover Util Environ Eff 2017;39(8):733–40. https://doi.org/10.1080/15567036.2013.783657.
[59] Lenis YA, Pérez JF, Melgar A. Fixed bed gasification of Jacaranda Copaia wood : effect of packing factor and oxygen enriched air. Ind Crop Prod 2016;84:166–75. https://doi.org/10.1016/j.indcrop.2016.01.053.
[60] Burbano HJ, Pareja J, Amell AA. Laminar burning velocities and flame stability analysis of H 2/CO/air mixtures with dilution of N2 and CO2. Int J Hydrogen Energy 2011;36(4):3232–42. https://doi.org/10.1016/j.ijhydene.2010.11.089.
[61] Monteiro E, Bellenoue M, Sotton J, Moreira NA, Malheiro S. Laminar burning velocities and Markstein numbers of syngas-air mixtures. Fuel 2010;89(8):1985–91. https://doi.org/10.1016/j.fuel.2009.11.008.
[62] Wang H, You X, Joshi AV, Davis SG, Laskin A, Law FECK. USC mech version II. High-temperature combustion reaction model of H2/CO/C1-C4. University of Delaware; 2007 [Online]. Available: http://ignis.usc.edu/USC_Mech_II.htm.
[63] Hernández JJ, Lapuerta M, Barba J. Flame stability and OH and CH radical emissions from mixtures of natural gas with biomass gasification gas. Appl Therm Eng 2013;55(1–2):133–9. https://doi.org/10.1016/j.applthermaleng.2013.03.015.
[64] Zhao Y, McDonell V, Samuelsen S. Influence of hydrogen addition to pipeline natural gas on the combustion performance of a cooktop burner. Int J Hydrogen Energy 2019;44(23):12239–53. https://doi.org/10.1016/j.ijhydene.2019.03.100.
[65] Bika AS. Synthesis gas use in internal combustion engines," Minnesota. 2010 [Online]. Available: https://conservancy.umn.edu/bitstream/handle/11299/99436/Bika_umn_0130E_11711.pdf?sequence=1&isAllowed=y.
[66] Paykani A, Chehrmonavari H, Tsolakis A, Alger T, Northrop WF, Reitz RD. Synthesis gas as a fuel for internal combustion engines in transportation. Prog Energy Combust Sci 2022;90:100995. https://doi.org/10.1016/j.pecs.2022.100995.
[67] Guangul FM, Sulaiman SA, Ramli A. Gasifier selection, design and gasification of oil palm fronds with preheated and unheated gasifying air. Bioresour Technol 2012;126:224–32. https://doi.org/10.1016/j.biortech.2012.09.018.
[68] Mahapatra S, Dasappa S. Experiments and analysis of propagation front under gasification regimes in a packed bed. Fuel Process Technol 2014;121:83–90. https://doi.org/10.1016/j.fuproc.2014.01.011.
[69] Williams FA. Combustion. In: Meyers RA, editor. Encyclopedia of physical science and technology. third ed. New York: Academic Press; 2003. p. 315–38. https://doi.org/10.1016/B0-12-227410-5/00123-X.
[70] Fiore M, Magi V, Viggiano A. Internal combustion engines powered by syngas: a review. Appl Energy 2020;276:115415. https://doi.org/10.1016/j.apenergy.2020.115415. June.
[71] Mohon Roy M, Tomita E, Kawahara N, Harada Y, Sakane A. Performance and emission comparison of a supercharged dual-fuel engine fueled by producer gases with varying hydrogen content. Int J Hydrogen Energy 2009;34(18):7811–22. https://doi.org/10.1016/j.ijhydene.2009.07.056.